

**DEVELOPMENT AND CHARACTERIZATION
OF LOPINAVIR AND VERAPAMIL HCL-
LOADED NANOSTRUCTURED LIPID
CARRIERS (NLC)**

ARSHAD ALI KHAN

UNIVERSITI SAINS MALAYSIA

2017

**DEVELOPMENT AND CHARACTERIZATION
OF LOPINAVIR AND VERAPAMIL HCL-
LOADED NANOSTRUCTURED LIPID
CARRIERS (NLC)**

by

ARSHAD ALI KHAN

**Thesis submitted in fulfillment of the requirement
for the degree of
Doctor of Philosophy**

April 2017

DEDICATION

This thesis is dedicated to my parents, who have given me invaluable educational opportunities, and to my wife, who has been my emotional anchor all the way.

ACKNOWLEDGMENT

All praise and thanks to my Lord who has granted me everything to complete the study. “Indeed! My success is only by ALLAH”.

First of all, my debt of gratitude and appreciation must go to my supervisor, Assoc. Prof. Dr. Yusrida Darwis for giving me her unmeasured guidance and encouragement throughout the course of the study. She has been a strong and extremely supportive adviser to me and has given me great freedom to complete my work. I feel proud to be a student of such a knowledgeable scientist who has given me all the support without any hesitation. It has been a great privilege working under her expert supervision.

I wish to express my deepest thanks the institute of postgraduate studies (IPS) for awarding me the elite USM fellowship during my PhD studies. This is indeed a biggest support during my whole research and thesis writing. Special thanks to Professor Dr. Munnavar Zubaid bin Abdul Sattar, the Dean of School of Pharmaceutical Sciences, Universiti Sains Malaysia.

Special thanks and appreciation also go to my co-supervisor, Dr. Vikneswaran a/l Murugaiyah for co-supervising me during every crucial step in my studies and I learned from him valuable things which I will always appreciate.

I am overwhelmingly thankful to my best colleagues and friends Ibrahim Abdulbaqi and Reem Abbou Assi for their genuine help and unlimited support throughout my study. They have been always supportive to me at times of both professionally and

personally. I would also like to extend my thanks to my special friends Nasir Hayat Khan, Amir Hayat Khan, Tauqeer Hussain Malhi, Yusra Tauqeer, Omaid Hayat Khan, Nagla, Yamuna Nair, Gabriel, Lee Fung, Lee Fen, Yasser Tabana, Asif Yazdani, Suman Bhatt, Jyotsna Sehrawat, Eshtiyag, Mohamed Lazhari, Abul Kalam, Arsalan Fehmi, Noor Hayat Sargana and Zubair Mahmood for their constant help and support. Deepest thanks to the laboratory staff from the School of Pharmaceutical Sciences, Mr Samsuddin Bakar, Mr Hafeez. All of them and their constant help are gratefully acknowledged.

Above all, I am enormously thankful to my loving parent, Sharafat Ali Khan and Suraiya Fatima for their absolute love and unconditional support throughout my study and life. My study would never be completed without their support. I have no enough words to thank their sacrifice and patience. I also thank to my great brothers Rashid Ali Khan and Shahid Ali Khan who was my biggest support during every step in my study. My loving thanks to my sister Sana Fatima for taking care of everything. My family is my greatest strength in my life and throughout my study.

Last, but certainly not least, a very special thanks to the strongest pillar of my life, my beloved wife Safia Akhtar Khan for her understanding and immense support during my study.

Arshad Ali Khan

TABLE OF CONTENTS

ACKNOWLEDGMENT	ii
TABLE OF CONTENTS	iv
LIST OF TABLES	xiv
LIST OF FIGURES	xvii
LIST OF PLATES	xxiii
LIST OF ABBREVIATION & SYMBOLS	xxiv
LIST OF APPENDICES	xxvi
ABSTRAK	xxviii
ABSTRACT	xxx
CHAPTER 1: INTRODUCTION AND LITRATURE REVIEW	1
1.1 Colloidal drug carriers	1
1.1.1 Microemulsions and nanoemulsions	2
1.1.2 Nanocapsules and polymeric nanoparticles	3
1.2 Lipid-based nanoparticles	4
1.2.1 Liposomes	4
1.2.2 Solid lipid nanoparticles (SLNs)	5
1.2.3 Nanostructured lipid carriers (NLCs)	5
1.2.3(a) NLCs composition	6
1.2.3(b) Methods of NLCs preparation	6
1.2.3(c) Characterization of NLCs	7
1.2.3(d) Stability of NLCs	7
1.2.3(e) Role of NLCs in different delivery system	7
1.2.3(f) NLCs versus SLNs	8
1.3 Lipid based nanoparticles as a carrier for oral drug delivery	9
1.4 The drug absorption of lipid-based nanoparticles via lymphatic circulation	10
1.5 Different routes for NLCs lymphatic uptake	14
1.5.1 Subcutaneous route for lymphatic delivery of NLCs	15
1.5.2 Pulmonary route for lymphatic delivery of NLCs	15
1.5.3 Intestinal route for lymphatic delivery of NLCs	16
1.6 <i>In vitro</i> models for studying lymphatic drug transport	18

1.6.1 <i>In vitro</i> cellular uptake study via Caco-2 cell monolayer model to evaluate the indirect lymphatic uptake of NLCs	18
1.6.2 Characteristics of Caco-2 cells	19
1.6.2(a) Tight junction	19
1.6.2(b) Drug transporters	19
1.6.2(c) Metabolic enzymes	20
1.6.2(d) Nuclear receptors	21
1.6.3 The usefulness and limitations of the Caco-2 cells monolayer	21
1.7 Types of lipids for preparing NLCs	23
1.7.1 Solid and liquid lipids	23
1.8 Selection of drugs	23
1.8.1 Lopinavir	24
1.8.1(a) Physicochemical properties	25
1.8.1(b) Pharmacology of lopinavir	26
1.8.1(c) Pharmacokinetic of lopinavir	28
1.8.1(d) Lopinavir nanoformulations	28
1.8.2 Verapamil hydrochloride	32
1.8.2(a) Physicochemical properties	33
1.8.2(b) Pharmacology of verapamil	34
1.8.2(c) Pharmacokinetic of verapamil	34
1.8.2(d) Verapamil nanoparticles	35
1.9 Problem statement of lopinavir and verapamil	36
1.10 Objectives of the present study	37
CHAPTER 2: DEVELOPMENT AND VALIDATION OF HPLC-UV METHOD FOR QUANTIFICATION OF LOPINAVIR	39
2.1 Introduction	39
2.2 Materials	42
2.3 Methods	42
2.3.1 Instrumentation	42
2.3.2 Selection of wavelength	43
2.3.3 Chromatographic conditions	43
2.3.4 Preparation of standard and quality control solutions	44

3.3.4 Optimization, statistical analysis and desirability function approach	64
3.3.5 The drug loading study	65
3.3.5(a) Separation of unloaded lopinavir from lopinavir-NLCs	65
3.3.5(b) Determination of entrapment efficiency, drug loading and yield	66
3.3.6 Statistical analysis	67
3.4 Result and discussion	67
3.4.1 Lopinavir-NLCs preparation	67
3.4.1(a) Screening of lipids	67
3.4.1(b) Screening of homogenization intensity	69
3.4.1(c) The 2 ⁴ full factorial design	70
3.4.2 Determination of drug loading, yield and encapsulation efficiency	85
3.5 Conclusion	86
CHAPTER 4: CHARACTERIZATION OF LYOPHILIZED LOPINAVIR-NLC FORMULATION	87
4.1 Introduction	87
4.2 Materials	88
4.3 Methods	88
4.3.1 Screening of cryoprotectant	88
4.3.2 Method of cryoprotectant addition	89
4.3.3 Estimation of mean particle size, PdI and zeta potential	90
4.3.4 Separation of free lopinavir from lopinavir-NLCs and Drug content estimation	90
4.3.5 Lopinavir release from NLCs	91
4.3.5(a) Preparation of simulated gastric fluid (SGF) without enzyme	91
4.3.5(b) Preparation of simulated intestinal fluid (SIF) without enzyme	91
4.3.5(c) <i>In vitro</i> release study	91
4.3.6 Differential scanning calorimetry (DSC)	93
4.3.7 Powder X-ray diffraction analysis (PXRD)	93
4.3.8 Transmission electron microscopy (TEM)	94
4.3.9 Scanning electron microscopy (SEM)	94
4.3.10 Short-term stability studies	94
4.4 Statistical analysis	95

4.5 Results and discussion	95
4.5.1 Screening of cryoprotectant and Freeze drying	95
4.5.2 <i>In vitro</i> release study	102
4.5.3 Differential scanning calorimetry (DSC)	106
4.5.4 Wide angle X-ray scattering	108
4.5.5 Transmission electron microscopy (TEM) and scanning electron microscopy (SEM)	109
4.5.6 Short-term stability studies	113
4.5.6(a) Physical appearance	113
4.5.6(b) Mean particle size, PdI and ZP	113
4.5.6(c) Drug content estimation	114
4.5.6(d) Shelf life estimation	117
4.5.6(e) <i>In vitro</i> release	118
4.6 Conclusion	122
CHAPTER 5: DEVELOPMENT AND VALIDATION OF A SIMPLE AND SENSITIVE HPLC-UV METHOD FOR DETERMINATION OF LOPINAVIR IN RAT PLASMA	123
5.1 Introduction	123
5.2 Materials	126
5.2.1 Collection of plasma	126
5.3 Methods	127
5.3.1 Chromatographic apparatus	127
5.3.2 Chromatographic conditions	127
5.3.3 Preparation of working standard solutions and quality control samples	127
5.3.4 Extraction method	128
5.3.5 Method validation	129
5.3.5(a) Specificity	129
5.3.5(b) Linearity	129
5.3.5(c) Limit of detection and limit of quantification	129
5.3.5(d) Precision and accuracy	130
5.3.5(e) Recovery	130
5.3.5(f) Stability	130
5.4 Result and discussion	132

5.4.1 Method development and optimization	132
5.4.2 Selection of internal standard	133
5.4.3 Extraction sample preparation	134
5.4.4 Method validation	135
5.4.4(a) Specificity	135
5.4.4(b) Linearity	136
5.4.4(c) Limit of detection and lower limit of quantification	138
5.4.4(d) Interday and intraday precision and accuracy	138
5.4.4(e) Recovery	138
5.4.4(f) Stability studies	139
5.5 Conclusion	140
CHAPTER 6: <i>IN VIVO</i> PHARMACOKINETIC STUDY OF LOPINAVIR- NLCS	141
6.1 Introduction	141
6.2 Materials and methods	142
6.2.1 Materials	142
6.2.2 Animals	142
6.2.3 Study protocol	143
6.2.4 Determination of lopinavir in plasma samples	146
6.2.5 Evaluation of pharmacokinetic parameters	147
6.2.6 Statistical analysis	147
6.3 Results and discussion	147
6.4 Conclusion	161
CHAPTER 7: DEVELOPMENT AND VALIDATION OF A REVERSED- PHASE HPLC-UV METHOD FOR QUANTIFICATION OF VERAPAMIL	162
7.1 Introduction	162
7.2 Materials	164
7.3 Methods	165
7.3.1 Instrumentation	165
7.3.2 Chromatographic conditions	165
7.3.3 Preparation of standard and quality control samples	165

7.3.4 Method validation	166
7.3.4(a) System suitability	166
7.3.4(b) Specificity	166
7.3.4(c) Linearity	166
7.3.4(d) Limit of detection and Limit of quantification	167
7.3.4(e) Precision and accuracy	167
7.3.4(f) Robustness	168
7.3.4(g) Stability study	168
7.3.5 Statistical analysis	168
7.4 Result and Discussion	169
7.4.1 Method development and optimization	169
7.4.2 Method validation	170
7.4.2(a) System suitability	170
7.4.2(b) Specificity	171
7.4.2(c) Linearity	173
7.4.2(d) Limit of detection and Limit of quantification	174
7.4.2(e) Interday and Intraday precision and accuracy	175
7.4.2(f) Robustness	175
7.4.2(g) Solution stability	177
7.5 Conclusion	177
CHAPTER 8: FORMULATION AND CHARACTERIZATION OF HYBRID VERAPAMIL-DEXTRAN-NANOSTRUCTURED LIPID CARRIERS	178
8.1 Introduction	178
8.2 Materials	182
8.3 Methods	182
8.3.1 Hybrid verapamil- dextran-NLCs (HVD-NLCs) preparation	182
8.3.2 Characterization of the NLCs	183
8.3.2(a) Particle size, polydispersity index (PDI) and Zeta potential (ZP)	183
8.3.2(b) Separation of free verapamil from HVD-NLCs	183
8.3.2(c) Determination of entrapment efficiency, drug loading and yield	184

8.3.3 Study of different formulation parameters using 2 ⁴ full factorial design	185
8.3.4 Optimization, statistical analysis and desirability function approach	186
8.3.5 Statistical analysis	187
8.4 Result and discussion	187
8.4.1 HVD-NLCs preparation	187
8.4.1(a) Selection of lipids	187
8.4.1(b) Screening of homogenization intensity	188
8.4.1(c) The 2 ⁴ full factorial design	188
8.4.1(d) Optimization of HVD-NLCs using the desirability function	201
8.4.1(e) Determination of drug loading and yield	202
8.5 Conclusion	203

CHAPTER 9: CHARACTERIZATION OF LYOPHILIZED HVD-NLCS FORMULATIONS **204**

9.1 Introduction	204
9.2 Materials	205
9.3 Methods	206
9.3.1 Separation of HVD-NLCs and screening of cryoprotectants	206
9.3.2 Method of cryoprotectant addition	207
9.3.3 Estimation of mean particle size, polydispersity index and zeta potential	208
9.3.4 Drug content estimation	209
9.3.5 Preparation of dissolution media and <i>in vitro</i> release study	210
9.3.5(a) Simulated gastric fluid (SGF) without enzyme	210
9.3.5(b) Simulated intestinal fluid (SIF) without enzyme	210
9.3.5(c) <i>In vitro</i> release study	210
9.3.6 Differential scanning calorimetry (DSC)	211
9.3.7 Powder X-ray diffraction analysis (PXRD)	211
9.3.8 Transmission electron microscopy (TEM)	212
9.3.9 Scanning electron microscopy (SEM)	212
9.3.10 Short-term stability studies	212
9.3.11 Statistical analysis	213
9.4 Results and discussion	213
9.4.1 Screening of cryoprotectant and Freeze drying	213

9.4.2 <i>In vitro</i> release study	219
9.4.3 Differential scanning calorimetry	221
9.4.4 Wide angle X-ray scattering (WAXS)	222
9.4.5 Transmission electron microscopy (TEM) and scanning electron microscopy (SEM)	224
9.4.6 Short-term stability studies	227
9.4.6(a) Physical appearance	227
9.4.6(b) Mean particle size, PdI and ZP	227
9.4.6(c) Drug content estimation	229
9.4.6(d) Shelf life estimation	231
9.4.6(e) <i>In vitro</i> release	232
9.5 Conclusion	235
CHAPTER 10: <i>IN VITRO</i> CELLULAR UPTAKE STUDY OF LOPINAVIR- NLCS AND HVD-NLCS THROUGH CACO-2 CELL MONOLAYER MODEL	237
10.1 Introduction	237
10.2 Materials	238
10.3 Instruments	238
10.4 Experimental design for cellular uptake study	239
10.4.1 Sample preparation	239
10.4.2 Experimentation	240
10.4.3 Statistical analysis	241
10.5 Results and discussion	242
10.5.1 Cellular uptake study of lopinavir-NLCs and free lopinavir- suspension	242
10.5.2 Cellular uptake study of HVD-NLCs, verapamil-solution and verapamil-dextran sulfate complex dispersion.	243
10.6 Conclusion	245
CHAPTER 11: SUMMARY AND GENERAL CONCLUSION	246
CHAPTER 12: SUGGESTIONS FOR FUTURE RESEARCH	249
12.1 Implementation of industry viable technique	249

12.2 <i>In vivo</i> pharmacokinetic study for verapamil-NLCs	249
12.3 Lymphatic uptake studies	250
12.4 Clinical study	250
REFERENCES	251
PUBLICATIONS AND PRESENTATIONS	306

LIST OF TABLES

	Page
Table 1.1	Formulations that have been used for lymphatic delivery. 13
Table 1.2	Example of liquid and solid lipids used in the NLCs formulation. 23
Table 1.3	The activities of HIV protease inhibitors leading to the identification of lopinavir, adapted from Sham et al. (1998) 27
Table 1.4	Solubility of verapamil in different solvents. 33
Table 2.1	System suitability analysis for lopinavir at 200 µg/mL. Mean ± SD, n=5. 50
Table 2.2	Lopinavir calibration curve results (Mean ± SD, n=5). 53
Table 2.3	Interday and intraday precision and accuracy. 54
Table 2.4	Evaluation of method robustness with 200 µg/mL lopinavir concentration. 55
Table 2.5	Evaluation of lopinavir solution stability at 25±2°C. 56
Table 3.1	Description of 2 ⁴ full factorial design. 64
Table 3.2	Observed responses (mean) in 2 ⁴ full factorial design for NLCs. 72
Table 3.3	Resulted data of the 2 ⁴ full factorial analysis of NLCs formulations. 73
Table 3.4	Regression results of the obtained responses for NLCs. 75
Table 3.5(a)	The drug incorporation (20 mg) in six selected NLCs formulations. 86
Table 3.5(b)	The drug incorporation (30 mg and 35) in three selected NLCs formulations. 86
Table 4.1	Screening of cryoprotectants. 99
Table 4.2(a)	Addition of cryoprotectant after homogenization process. 100
Table 4.2(b)	Addition of cryoprotectant during homogenization process. 101
Table 4.3	Stability characteristics of lyophilized Lopinavir-NLCs (LOP-3) in terms of particle size, PdI, ZP and drug content (n=3) in different storage conditions according to ICH Q 1 A (R2). 116
Table 5.1	Lopinavir calibration curve results. Mean ± SD, n=5. 137

Table 5.2	Interday and intraday precision and accuracy for lopinavir plasma samples.	138
Table 5.3	Lopinavir extraction recovery in rat plasma (Mean \pm SD, n=5).	139
Table 5.4	Lopinavir stability study in rat plasma at different stability conditions.	140
Table 6.1	The mean plasma concentration of lopinavir ($R_t = 6.5$ min) after intraduodenal administration of lopinavir-NLCs formulation (LOP-3) and free lopinavir suspension in rats. Mean \pm SD, n= 6.	149
Table 6.2	Values of T_{max} of individual rats for lopinavir-NLCs and free lopinavir-suspension.	157
Table 6.3	Values of C_{max} of individual rats for lopinavir-NLCs and free lopinavir-suspension.	158
Table 6.4	Values of area under the curve for 0-t, t-8 and 0-8 of lopinavir-NLCs in individual rats.	159
Table 6.5	Values of area under the curve for 0-t, t-8 and 0-8 of free lopinavir-suspension in individual rats.	159
Table 6.6	Values of $t_{1/2}$ (hrs.) of individual rats for lopinavir-NLCs and free lopinavir-suspension.	161
Table 6.7	Values of K_e (hrs-1) of individual rats for lopinavir-NLCs and free lopinavir-suspension.	161
Table 7.1	System suitability analysis for verapamil HCl at 100 $\mu\text{g/mL}$. Mean \pm SD, n=5.	171
Table 7.2	Verapamil HCl calibration curve results (Mean \pm SD, n=5).	173
Table 7.3	Interday and Intraday precision and accuracy.	175
Table 7.4	Evaluation of method robustness with 100 $\mu\text{g/mL}$ verapamil HCl concentration.	176
Table 7.5	Evaluation of verapamil HCl solution stability study at room temperature ($25\pm 2^\circ\text{C}$).	177
Table 8.1	Description of 2^4 full factorial design.	186
Table 8.2	Observed responses (mean) in 2^4 full factorial design for HVD-NLCs.	190

Table 8.3	Resulted data of the 2 full factorial analysis of HVD-NLCs formulations.	191
Table 8.4	Regression results of the obtained responses for HVD-NLCs.	193
Table 8.5	Obtained % drug loading and % yield in selected HVD-NLCs formulations obtained from the factorial design.	203
Table 9.1	Screening of different cryoprotectants on the basis of mean particle size and PDI.	216
Table9.2(a)	Results of mean particle size, PDI and encapsulation efficiency of selected HVD-NLCs formulations after lyophilization	217
Table9.2(b)	Trehalose was added during homogenization.	217
Table 9.3	Stability characteristics of lyophilized HVD-NLCs (VER-9) at terms of particle size, PDI, ZP and drug content (n=3) in different storage conditions according to ICH Q 1 A (R2).	230
Table 10.1	Incorporated and obtained lopinavir concentration in Caco-2 cell monolayer.	243
Table 10.2	Incorporated and obtained verapamil concentration in Caco-2 cell monolayer.	245

LIST OF FIGURES

	Page	
Figure 1.1	A Schematic transverse section of Peyer's patch, illustrating M cell transportation of lipid based formulation (nanostructured lipid carriers) to the lymphatic vessels. B Schematic diagram of the different mechanisms of the intestinal transport of lipid based formulation (nanostructured lipid carriers) through blood and lymphatic circulation. Adopted from Khan et al., (2013).	12
Figure 1.2	Drug transporters and metabolic enzymes present in Caco-2 cell monolayer.	20
Figure 1.3	Lopinavir, adapted from Sham et al. (1998).	25
Figure 1.4	Verapamil Hydrochloride.	32
Figure 2.1	Lopinavir UV absorption spectrum from 200 to 400 nm.	43
Figure 2.2	Chromatogram of pure lopinavir (10 mg/mL), placebo NLCs and lopinavir-NLCs (lopinavir 10 mg/mL) in SIF and SGF (Lopinavir retention time = 4.7 min).	51
Figure 2.3	Mean standard calibration curve of lopinavir	52
Figure 3.1	Separation of free lopinavir and lopinavir-NLCs using mini-column centrifugation method	66
Figure 3.2	The Screening of solid lipids and liquid lipids on the basis of lopinavir solubility.	69
Figure 3.3	Influence of high shear homogenization intensity (rpm) on mean particle sizes and polydispersity index of NLCs.	70
Figure 3.4	Response surface plot depicting the significant ($p < 0.05$) effect of homogenization time, solid lipid, liquid lipid concentration, surfactant concentration and interaction between AB, AC, AD, BC, BD and CD on particle size of NLCs.	78
Figure 3.5	Response surface plot depicting the significant ($p < 0.05$) effect of homogenization time, solid lipid, liquid lipid concentration and interactions between AC, BC, BD and CD on polydispersity index of NLCs.	80

Figure 3.6	Response surface plot depicting the significant ($p < 0.05$) effect of homogenization time, solid lipid, surfactant concentration and interactions between AD, BD and CD on zeta potential of NLCs.	82
Figure 3.7	Bar graphs displaying individual desirability of several responses and their combined overall desirability of selected NLCs formulations. (a) NLC-1, (b) NLC-4, (c) NLC-7, (d) NLC-8, (e) NLC-12 and (f) NLC-14.	84
Figure 4.1	(a) Cumulative percentage of lopinavir released in SGF (pH 1.2) for 24 hours, (b) Cumulative percentage of lopinavir released in PBS (pH 6.8) for 24 hours.	105
Figure 4.2	DSC thermograms of (a) Compritol 188, (b) Poloxamer 188, (c) Trehalose, (d) Lopinavir, (e) Physical mixture, (f) Blank, (g) LOP-3 formulation (with trehalose) and (h) LOP-3 formulation (without trehalose).	107
Figure 4.3	X-ray patterns of (a) Lyophilized lopinavir-NLCs formulation (LOP-3), (b) Lyophilized blank formulation, (c) Trehalose, (d) Lopinavir and (e) Compritol 888 ATO.	109
Figure 4.4	(a) TEM image of lopinavir-NLCs (LOP-3) before lyophilization, (b) SEM image of lopinavir-NLCs (LOP-3) without trehalose, and (c) SEM image of lopinavir-NLCs (LOP-3) with trehalose.	112
Figure 4.5	The shelf life estimation of lopinavir-NLCs (LOP-3) on the basis of total drug content.	117
Figure 4.6	<i>In vitro</i> release profile of LOP-3 at 2-8°C in (a) SIF and (b) SGF release media for 6 months.	119
Figure 4.7	(a) <i>In vitro</i> release profile of LOP-3 at 25°C in (a) SIF and (b) SGF release media for 6 months	120
Figure 4.8	(a) <i>In vitro</i> release profile of LOP-3 at 40°C in (a) SIF and (b) SGF release media for 6 months.	121
Figure 5.1	Structures of lopinavir and mefenamic acid (I.S.).	126

Figure 5.2	Representative chromatograms of (a) Blank rat plasma; (b) Plasma spiked with 1000 ng/ mL of lopinavir (6.57 min) and I.S. (4.1 min).	136
Figure 5.3	Mean standard calibration curve of lopinavir, n=5.	137
Figure 6.1	The chromatogram of I.S. (Mefenamic acid; retention time = 4.1) and lopinavir (retention time = 6.57) in rat plasma 30 min after the intraduodenal administration of lopinavir-NLCs.	148
Figure 6.2	Lopinavir plasma concentration profile over 24 hrs. in rat 1 after intraduodenal administration of lopinavir-NLCs.	149
Figure 6.3	Lopinavir plasma concentration profile over 24 hrs. in rat 2 after intraduodenal administration of lopinavir-NLCs.	150
Figure 6.4	Lopinavir plasma concentration profile over 24 hrs. in rat 3 after intraduodenal administration of lopinavir-NLCs.	150
Figure 6.5	Lopinavir plasma concentration profile over 24 hrs. in rat 4 after intraduodenal administration of lopinavir-NLCs.	151
Figure 6.6	Lopinavir plasma concentration profile over 24 hrs. in rat 5 after intraduodenal administration of lopinavir-NLCs.	151
Figure 6.7	Lopinavir plasma concentration profile over 24 hrs. in rat 6 after intraduodenal administration of lopinavir-NLCs.	152
Figure 6.8	Lopinavir plasma concentration profile over 24 hrs. in rat 1 after intraduodenal administration of free lopinavir-suspension.	152
Figure 6.9	Lopinavir plasma concentration profile over 24 hrs. in rat 2 after intraduodenal administration of free lopinavir-suspension.	153
Figure 6.10	Lopinavir plasma concentration profile over 24 hrs. in rat 3 after intraduodenal administration of free lopinavir-suspension.	153
Figure 6.11	Lopinavir plasma concentration profile over 24 hrs. in rat 4 after intraduodenal administration of free lopinavir-suspension.	154

Figure 6.12	Lopinavir plasma concentration profile over 24 hrs. in rat 5 after intraduodenal administration of free lopinavir-suspension.	154
Figure 6.13	Lopinavir plasma concentration profile over 24 hrs. in rat 6 after intraduodenal administration of free lopinavir-suspension.	155
Figure 6.14	Mean lopinavir plasma concentration profile over 24 hrs. in all rats after intraduodenal administration of lopinavir-NLCs and free lopinavir suspension.	155
Figure 7.1	Verapamil HCl UV absorption spectrum from 200 to 400 nm.	169
Figure 7.2	Chromatogram of pure verapamil HCl (100µg/mL), placebo NLCs and HVD-NLCs (Verapamil; 100µg/mL) in SIF and SGF. (Verapamil retention time = 2.8 min).	172
Figure 7.3	Mean standard calibration curve of verapamil HCl.	174
Figure 8.1	Chemical structures of (i) verapamil hydrochloride and (ii) dextran sulfate sodium.	180
Figure 8.2	Schematic illustration of HVD-NLCs composed of an electrostatic complex of water-soluble cationic drug verapamil and dextran sulfate.	181
Figure 8.3	Influence of high shear homogenization intensity (rpm) on mean particle sizes and polydispersity index of NLCs	188
Figure 8.4	Response surface plot depicting the significant ($p < 0.05$) effect of homogenization time, liquid lipid concentration, surfactant concentration and interaction between AC, BD and CD on particle size of HVD-NLCs.	196
Figure 8.5	Response surface plot depicting the significant ($p < 0.05$) effect of liquid lipid concentration and interactions between AC and CD on polydispersity index of HVD-NLCs.	197
Figure 8.6	Response surface plot depicting the significant ($p < 0.05$) effect of liquid lipid concentration, surfactant concentration and interactions between BD and CD on zeta potential of HVD-NLCs.	199

Figure 8.7	Response surface plot depicting the significant ($p < 0.05$) effect of homogenization time, liquid lipid concentration, surfactant concentration and interactions between AD and BD on entrapment efficiency of verapamil in HVD-NLCs.	200
Figure 8.8	Bar graphs displaying individual desirability of several responses and their combined overall desirability of selected HVD-NLCs formulations. (a) VER-9, (b) VER11, (c) VER-13 and (d) VER-15.	202
Figure 9.1	(a) Cumulative percentage of verapamil released in SGF (pH 1.2) for 72 hours, (b) Cumulative percentage of verapamil released in SIF (pH 6.8) for 72 hours.	220
Figure 9.2	DSC thermograms of (a) Compritol 888 ATO, (b) Poloxamer 188, (c) Verapamil HCl, (d) Dextran sulfate, (e) Trehalose, (f) Verapamil HCl and dextran sulfate physical mixture, (g) Physical mixture, (h) Lyophilized blank formulation and (i) HVD-NLCs formulation (VER-9).	222
Figure 9.3	X-ray patterns of (a) Lyophilized HVD-NLCs formulation (VER-9), (b) Lyophilized blank formulation, (c) Trehalose, (d) Dextran sulfate, (e) Verapamil HCl and (f) Compritol 888 ATO.	224
Figure 9.4	TEM image of HVD-NLCs before lyophilization.	225
Figure 9.5	SEM images of LPV-NLCs with and without trehalose.	226
Figure 9.6	The shelf life estimation of HVD-NLC formulation (VER-9) on the basis of drug content.	231
Figure 9.7	<i>In vitro</i> release profile of VER-9 at 2-8°C in SIF for 6 months, (b) <i>In vitro</i> release profile of VER-9 at 2-8°C in SGF for 6 months.	233
Figure 9.8	(a) <i>In vitro</i> release profile of VER-9 at 25°C in SIF for 6 months, (b) <i>In vitro</i> release profile of VER-9 at 25°C in SGF for 6 months.	234
Figure 9.9	(a) <i>In vitro</i> release profile of VER-9 at 40°C in SIF for 6 months, (b) <i>In vitro</i> release profile of VER-9 at 40°C in SGF for 6 months.	235

Figure 10.1 Illustration of Caco-2 cell monolayer uptake experimentation in 48 well plate.

241

LIST OF PLATES

	Page
Plate 6.1 Demonstration of duodenum after small incision in the abdomen.	210
Plate 6.2 Intraduodenal administration of test sample with a hypodermic syringe	210
Plate 6.3 The incision was sutured back after sample administration	211

LIST OF ABBREVIATION & SYMBOLS

ANOVA	Analysis of Variance
AUC	Area Under Curve
C_{\max}	Maximum plasma drug concentration
DSC	Differential Scanning Calorimetry
e.g.	<i>exempli gratia</i>
GRAS	Generally recognized as safe
HPLC	High Performance Liquid Chromatography
hr	Hour
ICH	International Conference on Harmonization
ID	Internal Diameter
K_e	Elimination rate constant
Kg	Kilogram
LOD	Limit of Detection
LOQ	Limit of Quantification
M	Molar
mg	Milligram
min	Minute
mm	Millimeter
mL	Milliliter
nm	Nanometer
N	Theoretical plates
ng	Nanogram
NLCs	Nanostructured lipid carriers
o/w	Oil in water
PCS	Photon correlation spectroscopy
PdI	Polydispersity index
QC	Quality Control
RE	Relative Error
RH	Relative Humidity
rpm	Rotation per minute
RSD	Relative Standard Deviation
RSM	Response surface methodology

SD	Standard deviation
SEM	Scanning Electron Microscopy
Sec	Second
SLNs	Solid lipid nanoparticles
SMEDDS	Self microemulsifying drug delivery system
SNEDDS	Self nanoemulsifying drug delivery system
TEM	Transmission Electron Microscopy
T _{max}	Time taken to reach maximum plasma concentration
t _{1/2}	Half life
USFDA	United States Food and Drug Administration
USP	United States Pharmacopoeia
UV	Ultraviolet
v/v	Volume by Volume
w/v	Weight by Volume
XRD	X-ray powder diffraction
ZP	Zeta potential
µg/mL	Microgram per milliliter
µL	Microliter
°C	Degree centigrade

LIST OF APPENDICES

		Page
Appendix A1	<i>In vitro</i> release profile of lopinavir from selected formulations and free drugs	304
Appendix A2	<i>In vitro</i> release profile of lopinavir in SIF from formulation Lop-3 at 5°C storage throughout the stability study.	306
Appendix A3	<i>In vitro</i> release profile of lopinavir in SGF from formulation Lop-3 at 5°C storage throughout the stability study.	307
Appendix A4	<i>In vitro</i> release profile of lopinavir in SIF from formulation Lop-3 at 25°C storage throughout the stability study.	308
Appendix A5	<i>In vitro</i> release profile of lopinavir in SGF from formulation Lop-3 at 25°C storage throughout the stability study.	309
Appendix A6	<i>In vitro</i> release profile of lopinavir in SIF from formulation Lop-3 at 40°C storage throughout the stability study.	310
Appendix A7	<i>In vitro</i> release profile of lopinavir in SGF from formulation Lop-3 at 40°C storage throughout the stability study.	311
Appendix B1	<i>In vitro</i> release profile of verapamil from formulation VER-9, VER-11 and free drug.	312
Appendix B2	<i>In vitro</i> release profile of verapamil from formulation VER-9 in SGF at 5°C storage throughout the stability study.	314
Appendix B3	<i>In vitro</i> release profile of verapamil from formulation VER-9 in SIF at 5°C storage throughout the stability study.	315

Appendix B4	<i>In vitro</i> release profile of verapamil from formulation VER-9 in SGF at 25°C storage throughout the stability study.	316
Appendix B5	<i>In vitro</i> release profile of verapamil from formulation VER-9 in SIF at 25°C storage throughout the stability study.	317
Appendix B6	<i>In vitro</i> release profile of verapamil from formulation VER-9 in SGF at 40°C storage throughout the stability study.	318
Appendix B7	<i>In vitro</i> release profile of verapamil from formulation VER-9 in SIF at 40°C storage throughout the stability study.	319

**PEMBANGUNAN DAN PENCIRIAN PEMBAWA LIPID NANOSTRUKTUR
(NLC) BERMUATAN LOPINAVIR DAN VERAPAMIL HCL**

ABSTRAK

Tujuan kajian ini adalah untuk menyediakan pembawa lipid nanostruktur (NLC) lopinavir (tidak larutair) dan verapamil (larut air). NLC disediakan dengan menggunakan lipid pepejal (compritol 888 ATO), lipid cecair (asid oleik), dan surfaktan (poloxamer 188 dan Tween 80). Formulasi NLC disediakan dengan menggunakan teknik penyeragaman ricih tinggi. Reka bentuk faktorial 2^4 penuh digunakan dalam mengoptimumkan formulasi. Kesan empat pembolehubah tidak bersandar, termasuk masa penyeragaman, kepekatan lipid pepejal, cecair lipid dan surfaktan ke atas pembolehubah bersandar iaitu saiz zarah, indeks polisebaran (PDI), potensi zeta (ZP) dan kecekapan % pemerangkapan (EE) telah dikaji. Formulasi NLC bermuatan drug terpilih di beku-kering menggunakan trehalose sebagai agen pelindung. NLC bermuatan lopinavir beku-kering optimum (LOP-3) mempunyai purata saiz zarah, PDI, ZP dan % EE masing-masing 286.8 ± 1.3 nm, 0.413 ± 0.017 , -48.6 ± 0.888 mV dan $87.83 \pm 2.04\%$. NLCS bermuatan verapamil beku-kering optimum (VER-9) mempunyai saiz zarah, PDI, ZP dan % EE masing-masing 192.29 ± 2.98 nm, 0.553 ± 0.075 , -48.8 ± 0.569 dan $93.26 \pm 2.66\%$. Kajian pelepasan *in vitro* formulasi optimum LOP-3 dan VER-9 dalam bendalir simulasi gastrik (pH 1.2) dan bendalir simulasi usus (pH 6.8) masing-masing menunjukkan pelepasan pantas dan pelepasan bertahan. Kajian diferensial imbasan kalorimetri kedua-dua formulasi (LOP-3 dan VER-9) menunjukkan tiada interaksi kimia antara drug, lipid dan eksipien lain. Kajian sudut lebar X-ray penyerakan mengesahkan keadaan amorfus drug yang dimuatkan dalam kedua-dua formulasi LOP-3 dan VER-9. Imej TEM kedua-dua

formulasi LOP-3 dan VER-9 menunjukkan nanopartikel berbentuk bukan sfera dengan masing-masing saiz <100 dan <200 nm. Imej SEM menunjukkan bahawa trehalose mengurangkan agregasi formulasi LOP-3 dan VER-9. Kajian *in vitro* pengambilan selular formulasi LOP-3, VER-9 dan ampaiian drug bebas yang dilakukan menggunakan Caco-2 garis sel, menunjukkan pengambilan drug yang lebih tinggi daripada formulasi NLC berbanding ampaiian drug bebas. Profil farmakokinetik formulasi LOP-3 berikutan pemberian intraduodenal kepada tikus jantan Wistar menunjukkan bahawa bioavailabiliti relatif LOP-3 telah meningkat sebanyak 12.25 kali ganda berbanding ampaiian lopinavir bebas. Kajian kestabilan jangka pendek formulasi LOP-3 dan VER-9 dilakukan pada empat masa (0, 1, 3 dan 6 bulan) dan pada tiga keadaan penyimpanan yang berbeza ($5^{\circ}\text{C} \pm 3^{\circ}\text{C}$, $25^{\circ}\text{C} \pm 2^{\circ}\text{C} / 60\% \text{RH} \pm 5\% \text{RH}$ dan $40^{\circ}\text{C} \pm 2^{\circ}\text{C} / 75\% \text{RH} \pm 5\% \text{RH}$). Formulasi LOP-3 dan VER-9 stabil pada penyimpanan sejuk ($5^{\circ}\text{C} \pm 3^{\circ}\text{C}$). Jangka hayat formulasi LOP-3 dan VER-9 masing-masing adalah 18.84 dan 30.55 bulan. Kesimpulan, NLC bermuatan lopinavir dan verapamil HCl telah berjaya dibangunkan untuk penghantaran oral dan boleh sebagai alternatif kepada produk yang ada dipasaran untuk meningkatkan bioavailability oral.

**DEVELOPMENT AND CHARACTERIZATION OF LOPINAVIR AND
VERAPAMIL HCL-LOADED NANOSTRUCTURED LIPID CARRIERS
(NLC)**

ABSTRACT

The aim of the present study was to prepare nanostructured lipid carriers (NLCs) of lopinavir (water insoluble) and verapamil (water soluble). NLCs were prepared using solid lipid (e.g. compritol 888 ATO), liquid lipid (e.g. oleic acid), and surfactants (e.g. poloxamer 188 and tween 80). The NLCs formulation was prepared using a high shear homogenization technique. The 2⁴ full factorial design was applied in the optimization of formulations. The effect of four independent variables, including homogenization time, solid lipid, liquid lipid and surfactant concentrations on the dependent variables, namely particle size, poly dispersity index (PDI), zeta potential (ZP) and % entrapment efficiency (EE) were studied. The selected drug loaded NLCs formulations were freeze-dried using trehalose as a cryoprotectant. The optimized freeze-dried lopinavir loaded NLCs (LOP-3) had mean particle size, PDI, ZP and % EE of 286.8±1.3 nm, 0.413±0.017, -48.6±0.888 mV and 87.83 ± 2.04 %, respectively. The optimized freeze-dried verapamil loaded NLCs (VER-9) had mean particle size, PDI, ZP and % EE of 192.29 ± 2.98 nm, 0.553 ± 0.075, -48.8±0.569 and 93.26 ± 2.66 % respectively. *In vitro* release studies of optimized LOP-3 and VER-9 formulations in simulated gastric fluid (pH 1.2) and simulated intestinal fluid (pH 6.8) showed a burst and sustained release, respectively. The Differential scanning calorimetry study of both formulations (LOP-3 and VER-9) revealed the absence of chemical interaction between the drug, lipids and other formulation excipients. The wide angle X-ray scattering study revealed the amorphous state of loaded drug in both LOP-3 and VER-

9 formulations. TEM image of both LOP-3 and VER-9 formulations showed non-spherical shape nanoparticles with size of <100 and <200 nm respectively. SEM images showed that trehalose reduced aggregation of LOP-3 and VER-9 formulations. The *In vitro* cellular uptake studies of LOP-3, VER-9 formulations and free drug suspensions performed using Caco-2 cell line showed higher drug uptake from the NLCs formulations than the free drug suspension. The pharmacokinetic profile of LOP-3 formulation following intraduodenal administration of the formulation to male Wistar rats showed that the relative bioavailability of LOP-3 was increased by 12.25-fold compared to the free lopinavir suspension. The short term stability studies were performed for LOP-3 and VER-9 formulations at four time points (0, 1, 3 and 6 months) and three different storage conditions ($5^{\circ}\text{C} \pm 3^{\circ}\text{C}$, $25^{\circ}\text{C} \pm 2^{\circ}\text{C}/60\% \text{RH} \pm 5\% \text{RH}$ and $40^{\circ}\text{C} \pm 2^{\circ}\text{C}/75\% \text{RH} \pm 5\% \text{RH}$). The LOP-3 and VER-9 formulations were found stable in refrigerated storage condition ($5^{\circ}\text{C} \pm 3^{\circ}\text{C}$). The shelf life of LOP-3 and VER-9 formulations were 18.84 and 30.55 months respectively. In conclusion, lopinavir and verapamil HCl loaded NLCs were successfully developed for oral delivery and could be an alternative to the available marketed products to improve the oral bioavailability.

CHAPTER 1

INTRODUCTION AND LITRATURE REVIEW

1.1 Colloidal drug carriers

The new technologies employed in drug discovery lead to find many new powerful substances. The development of new drugs alone is not sufficient to ensure progress in drug therapy. The main and common problems of new drug molecules are poor water solubility and inadequate bioavailability. The size reduction is the method of choice to enhance the solubility and hereafter the bioavailability of poorly water-soluble drugs. However, this method only suitable for class II and IV drugs of biopharmaceutical classification system (BCS). Therefore, to develop a drug carrier system has become an increasing demand to overcome these obstacles.

The ideal properties of the developed carrier system should have higher drug loading capacity, controlled release, possibility of drug targeting and free of acute and chronic toxicity. It should also offer chemical and physical stability for the loaded drug. The feasibility of production scaling up with reasonable overall costs should be available (Barratt, 2000; Mehnert & Mäder, 2001; Mainardes & Silva, 2004; Roger et al., 2010).

The colloidal carriers system, particularly those in the nanosize range, have been increasingly investigated in the last several years because they can fulfill the required properties mentioned above (van de Waterbeemd, 1998; Dressman & Reppas, 2000).

1.1.1 Microemulsions and nanoemulsions

Microemulsions are optically isotropic, transparent or translucent, low-viscous, single-phase liquid solutions. They are thermodynamically stable bicontinuous systems, which are essentially composed of water, oil, surfactant and co-surfactant (Cortesi & Nastruzzi, 1999; Heuschkel et al., 2008; Santos et al., 2008; Flores et al., 2016). Microemulsions exhibit better solubilizing capacities for both hydrophilic and lipophilic drugs than micellar solutions. Due to the high surfactant concentration in microemulsions, they are usually limited to dermal and peroral applications.

In the 1950's, nanoemulsions were introduced for the purposes of parenteral nutrition. They are heterogeneous systems composed of two immiscible liquids in which one liquid is dispersed as droplets in the other one and the obtained liquid-liquid dispersion shows thermodynamic instability (Yukuyama et al., 2016; Ganta et al., 2014). Nanoemulsions have been used since some decades as drug carriers for lipophilic actives. Several pharmaceutical products based on nanoemulsion system have been introduced to the market e.g. Diazepam Lipuro[®], Etomidat Lipuro[®], Stesolid[®], Valium[®], Diazemuls[®] and NANOSTAT[™] (Chime et al., 2014).

The advantages of nanoemulsions over microemulsions in terms of drug delivery are the reduction of the local and systemic side effects, for example lesser pain during injection and hemolytic activity caused by the high emulsifying agent concentration in microemulsions (Yukuyama et al., 2016). However, the lipophilic loaded drug can move from the oil droplets to the aqueous medium due to their partition effects and hence, stability problems arise (Dingler et al., 2008). Furthermore, the possibility of

controlled drug release from nanoemulsions is limited due to the high mobility of the loaded drug which is dissolved in the oily phase. Ammar et al., (2009) highlighted a rapid release of the drugs from nanoemulsions.

1.1.2 Nanocapsules and polymeric nanoparticles

Nanocapsules consist of a barrier made from polymers between the core (usually oil) and the aqueous surrounding environment. Interfacial polymerization and solvent displacement methods are often used for nanocapsules preparation (Letchford & Burt, 2007; Kothamasu et al., 2012). Polymers used in the formulation of nanocapsules include cellulose derivatives, poly methylidene malonate, poly alkylcyanoacrylates, polyanhydrides, polyorthoesters and polyesters for example poly glycolic acid, poly lactid acid and poly ϵ -caprolactone and their copolymers (Mora-Huertas et al., 2010). Various procedures are applied for polymeric nanoparticles production e.g. solvent evaporation, coacervation technique, interfacial polymerization, degradation by high-shear forces (high pressure homogenization or micro fluidization) and natural proteins or carbohydrates denaturation or desolvation (Mora-Huertas et al., 2010; Kothamasu et al., 2012).

In comparison to liposomes and emulsions, the presence of polymeric barrier in nanocapsules and solid polymeric matrix in polymeric nanoparticles can provide more protection to the loaded drug molecules (Mayer, 2005; Anton et al., 2008; Mora-Huertas et al., 2010). Currently, these carriers have come in the market in the name of some pharmaceutical products e.g. Enantone Depot[®], Decapeptyl[®] and Gonapeptyl Depot[®].

1.2 Lipid-based nanoparticles

1.2.1 Liposomes

Liposomes consist of single or multi lipid bilayers of amphiphilic lipids, such as phospholipids, glycolipids and cholesterol (Allen & Cullis, 2013). Liposomes were described in 1965 by Bangham et al. as a cell membrane model (Bangham, 1992). Later on they were used as a carrier system and were introduced to the cosmetic market by Dior in 1986. The first topical liposomal pharmaceutical product in the brand name of Pevaryl[®]-Lipogel was produced by Cilag. Comprehensive biodisposition studies showed the superiority of the liposomes over the commercial Pevaryl gel, lotion and cream forms. The liposomal products resulted in an increase in drug concentration in the epidermis (7-9 folds), at the site of action (Touitou et al., 1994). The liposomal products displayed less toxicity in contrast to the conventional formulations of the same active pharmaceutical ingredients (Fassas & Anagnostopoulos, 2005; Akbarzadeh et al., 2013). The liposomes size ranges in between few nanometers to some micrometers. There are many methods to prepare the liposomes, e.g. solvent dispersion, detergent dialysis and mechanical dispersion (Elsayed et al., 2007; Samad et al., 2007; Akbarzadeh et al., 2013). The hydrophilic and lipophilic drugs can be encapsulated into the liposomes and due to liposomal composition, this carrier system are also acceptable for intravenous dosage form (Müller et al., 2000; Allen & Cullis, 2013;). During storage, it shows some physical and chemical instability due to unsaturated fatty acid oxidation and phospholipids ester binding hydrolysis. Moreover, due to lack of proper production methods, it cannot produce on large scale easily. All of these points make liposomes not optimal as a pharmaceutical carrier system. To overcome some of the liposomes drawbacks, niosomes were developed. The niosomes

was prepared by saturated hydrocarbon chains with intramolecular ether bindings that increases its chemical stability (Choi & Maibach, 2005; Allen & Cullis, 2013).

1.2.2 Solid lipid nanoparticles (SLNs)

SLNs are prepared by substituting the oil (liquid lipid) of oil in water emulsion by a solid lipid or a blend of solid lipids. This mixture produced solid nanoparticles which stay solid at both body and room temperature (Lucks Stefan, 1993; Parhi & Suresh, 2012). SLNs are comprised of 0.1%w/w to 30%w/w of solid lipid with respect to the amount of whole formulation and usually it stabilized with 0.5%w/w to 5%w/w of surfactant with respect to lipid content. The size of SLNs ranged in submicron region, i.e. extending from around 40 nm to 1 micron (Lucks Stefan, 1993; Parhi & Suresh, 2012).

Moreover, after the preparation at least a part of the solid lipid in SLNs crystallizes in a higher energy modification (α or β'). During storage, these modifications can transform to the low energy, more ordered β modification. Due to this high degree of order, the number of imperfections in the SLNs crystal lattice is small, this leads to drug expulsion (Mehnert & Mäder, 2001; Müller et al., 2002b).

1.2.3 Nanostructured lipid carriers (NLCs)

NLCs have been developed to overcome the drawbacks associated with SLNs. They are considered to be the second generation of lipid nanoparticles. Compared to SLNs, NLCs show a higher loading capacity for active compounds by creating a less ordered solid lipid matrix, i.e. by blending a liquid lipid with the solid lipid, a higher particle

drug loading can be achieved. Therefore, the NLCs have an increased drug loading capacity in comparison to SLNs and the possibility of drug expulsion during storage is less (Müller et al., 2002a; Müller et al., 2002b; Saupe et al., 2005; Naseri et al., 2015; Khan S et al., 2015). NLCs have also a lower water content of the particle suspension and a less tendency of unpredictable gelation (Müller et al., 2002a; Naseri et al., 2015).

1.2.3(a) NLCs composition

NLCs are prepared using combinations of solid and liquid lipids (oils). Herein solid lipids and liquid lipids are mixed together at ratio of 70:30 to 99.9:0.1 to obtain the controlled structured particle matrix. The obtained blends are solid at body and room temperature rather than present as oil (liquid lipids) in the mixture (Müller et al., 2000). The total solid content of NLCs can be enhanced up to 95% (Selvamuthukumar & Velmurugan, 2012)

1.2.3(b) Methods of NLCs preparation

Various methods have been used for the preparation of NLCs. The methods are microemulsion technique (Gupta et al., 2014), emulsification-solvent evaporation (Andalib et al., 2012), multiple emulsion technique (Selvamuthukumar & Velmurugan, 2012), solvent injection (or solvent displacement) (Tiwari & Pathak, 2011), ultrasonication (Uprit et al., 2013), phase inversion (Ming Sun et al., 2014) (Ming Sun et al., 2014), membrane contractor technique (Thatipamula et al., 2011), high-pressure homogenization (Shangguan et al., 2014) and high-shear homogenization (Ustündağ-Okur et al., 2014). High shear-homogenization is very common technique for lipid based nanoformulations. It shows several benefits over

other techniques for example, easy production scale-up, lesser process time and avoidance of organic solvent. For these reasons, it is widely accepted in several productions areas such as pharmaceutical and food industry.

1.2.3(c) Characterization of NLCs

Characterization of NLCs may be a serious challenge because of the small size of the particles resulting in the complexity of the system. Therefore, characterization of the NLCs may be an essential requisite for the management of the quality of the product. Many parameters need to be considered that have direct impact on the stability and release kinetics of NLCs such as particle size, polydispersity index and zeta potential.

1.2.3(d) Stability of NLCs

Among the hurdles in lipid based nanoparticles development, the long-term instability of lipid based nanoparticles dispersions is undoubtedly a major concern. In order to prolong the physical and chemical stability of the NLCs the water removal is a necessary step. The best common method in the pharmaceutical field is freeze drying which allows to change aqueous formulation into dried formulation for sufficient stability during storage (Franks, 1998; Varshosazet et al., 2012). Pharmaceutically, it is also known as lyophilization. It removes water from the frozen sample via sublimation and then desorption of that vapors take place under vacuum.

1.2.3(e) Role of NLCs in different delivery system

NLCs are used as biocompatible carriers for several types of drugs intended for pharmaceutical, cosmetic, and biochemical purposes. During the last one decade

different drugs or active substances have been entrapped into NLCs like lipophilic, hydrophilic molecules, including labile compounds, such as proteins and peptides. Their main feature is that they are prepared with physiologically well-tolerated lipids. The wide range of surfactants and cosurfactants available for the production of such particles make these carriers highly suitable for distinct applications like for topical, oral, parenteral, inhalational and ocular administration.

1.2.3(f) NLCs versus SLNs

As mentioned previously NLCs overcome the disadvantages associated with SLNs, in other words, they provide higher drug loading, faster release rate and storage stability due to a use of blend of solid lipid and liquid lipid in their formulations. Several comparative studies have been documented in literature in which NLCs have served as a better carrier than SLNs. For example, in a study between SLNs and NLCs of simvastatin, it was observed that entrapment efficiency of the drug was improved in NLCs (93.33%) when compared with SLNs (75.81%) due to creation of extra space for loading by liquid lipid (Tiwari & Pathak, 2011). Also, the *in vitro* release patterns in both SLNs and NLCs were similar but NLCs displayed high-percent cumulative drug release in comparison to SLNs in 55 h. A lesser mobility of drug in SLNs (a crystallized system) in comparison to NLCs (disordered arrangement) was responsible for the slower release of drug. Differential scanning calorimetric analysis showed decreased recrystallization index of NLCs in comparison to solid lipids and physical mixture of solid lipid and liquid lipid favoring the formation of disordered arrangement and reduced capacity of solid lipids to recrystallize suggesting their higher long-term stability. The results of *in vivo* studies also suggested NLCs to be superior as they exhibited 2.29-fold increase in oral bioavailability when administered to mice. Similar

results were also noted with lovastatin-loaded NLCs. Study of partitioning behavior of lovastatin in pure solid lipid and mixtures of solid lipid and liquid lipid also depicted higher partitioning of drug in the lipid phase consisting of a mixture of solid lipid (Precirol ATO 5) and liquid lipid (squalene) thus suggesting that higher solubility of drug was favored by the presence of liquid lipid (Chen et al., 2010). Another report on progesterone (Yuan, Wang, et al., 2007) and domperidone-loaded (Thatipamula et al., 2011) SLNs and NLCs also suggested the NLCs as a better vehicle in respect of drug loading and release rate (Poonia, Kharb, Lather, & Pandita, 2016).

1.3 Lipid based nanoparticles as a carrier for oral drug delivery

Lipid based nanoparticles for example SLNs and NLCs can be given by oral route in tablet, capsules, pellets, dispersions and as lyophilized powders ready for reconstitution (Mehnert & Mäder, 2001). The GIT stability of lipid nanoparticles has to be comprehensively studied, the acidic pH and elevated ionic strength in the upper GIT could result in lipid nanoparticles aggregation. So, to verify this, some authors investigated different lipid nanoparticle formulations behavior in simulated gastric fluids. They observed that zeta potential of a minimum 8-9 mV might hinder lipid nanoparticles aggregation (Zimmermann & Müller, 2001). Furthermore, to optimize the release profile of lipid nanoparticles, the knowledge of enzymatic degradation of lipids during *in vivo* drug release studies is essential (Olbrich & Müller, 1999). Since, *in vivo* release media contain lipolytic enzyme (pancreatic lipase) and drug release take place by lipid matrix degradation and solid phase diffusion process. While, *in vitro* drug release take place by solid phase diffusion, due to absence of lipolytic enzyme. Olbrich & Müller (1999), established an enzymatic degradation assay of SLNs using a lipase/colipase complex. In that, it shown that the degradation velocity depends on

the composition of the lipid matrix. In general, degradation velocity increased with decreasing length of the fatty acid chain length when using glycerides as lipid matrix. In addition, the degradation of SLNs based on waxes (e.g. cetylpalmitate) was found to be slower compared to glyceride matrices (Olbrich & Müller, 1999). A prerequisite for the degradation of lipid nanoparticles after oral administration is the anchoring of the lipase/ colipase complex onto the particle surface. Therefore, it was expected that not only the composition of the lipid matrix, but also the nature of the stabilizing surfactant layer would be a determining factor for degradation (Olbrich & Müller, 1999). Compounds such as cholic acid sodium salt are known to promote the anchoring of the lipase colipase complex on surfaces (Borgström, 1975). Sterically stabilizing polymers such as the Poloxamer series are known to prevent or to hinder the absorption of large molecules such as proteins (Blunk et al., 1993).

1.4 The drug absorption of lipid-based nanoparticles via lymphatic circulation

The lymphatic system is part of the circulatory system and is comprised of an intricate network of conduits that carry a clear fluid called lymph. The primary functions of the lymphatic system are to maintain the body's water balance by returning extracellular fluid that has leaked out into the interstitial space back to the systemic circulation and to transport immune cells to the lymph nodes (Iqbal & Hussain, 2009; Miteva et al., 2010). Further, the lymphatic system has specialized roles in specific areas because of its nonuniform structure and function throughout the body. It plays an essential role in absorption of long- chain fatty acids, triglycerides, cholesterol esters, lipid soluble vitamins, and xenobiotics (Iqbal & Hussain, 2009). Drug delivery via the lymphatic system has several major advantages, including circumventing first-pass metabolism in the liver and targeting drugs to diseases that spread through the lymphatic system

(eg, certain types of cancer and human immunodeficiency virus). The lymphatic system also plays an active role in disseminating metastatic cancer cells and infectious agents throughout the body. Cancer cells use the lymph nodes as a reservoir to spread to other areas of the body (Sleeman, 2000, 2006; Pantel & Brakenhoff, 2004; Lee et al., 2005; Iqbal & Hussain, 2009).

There are three ways to deliver drugs through the intestinal lymphatic vessels (Muranishi et al., 1997; Porter & Charman, 1997). First, lymphatic capillaries are comprised of single-layered, nonfenestrated endothelial cells. These cells are arranged in a highly gapped and overlapped manner to form a porous wall in the lymphatic vasculature, which allows for macromolecular targeting to the lymphatic system. Therefore, increased absorption of hydrophilic macromolecules and macroconjugates is possible by opening up the paracellular route with the help of an absorption enhancer (Hiroshi et al., 1981). Secondly, gut-associated lymphoid tissue consists of either isolated or aggregated lymphoid follicles that form Peyer's patches, which provide an entry point for drug to the lymphatics (Figure 1.1 A) (Eldridge et al., 1990; Hawley, Davis, & Illum, 1995; Beier & Gebert, 1998; Wells & Mercenier, 2008). Finally, the primary route for lipid transport is through the intestinal walls via transcellular absorption, paracellular transport, P-glycoprotein, and cytochrome P450 inhibition. Increased production of chylomicrons is associated with delivery of lipophilic compounds into the lymphatic system (Figure 1.1 B) ((Porter & Charman, 1997).

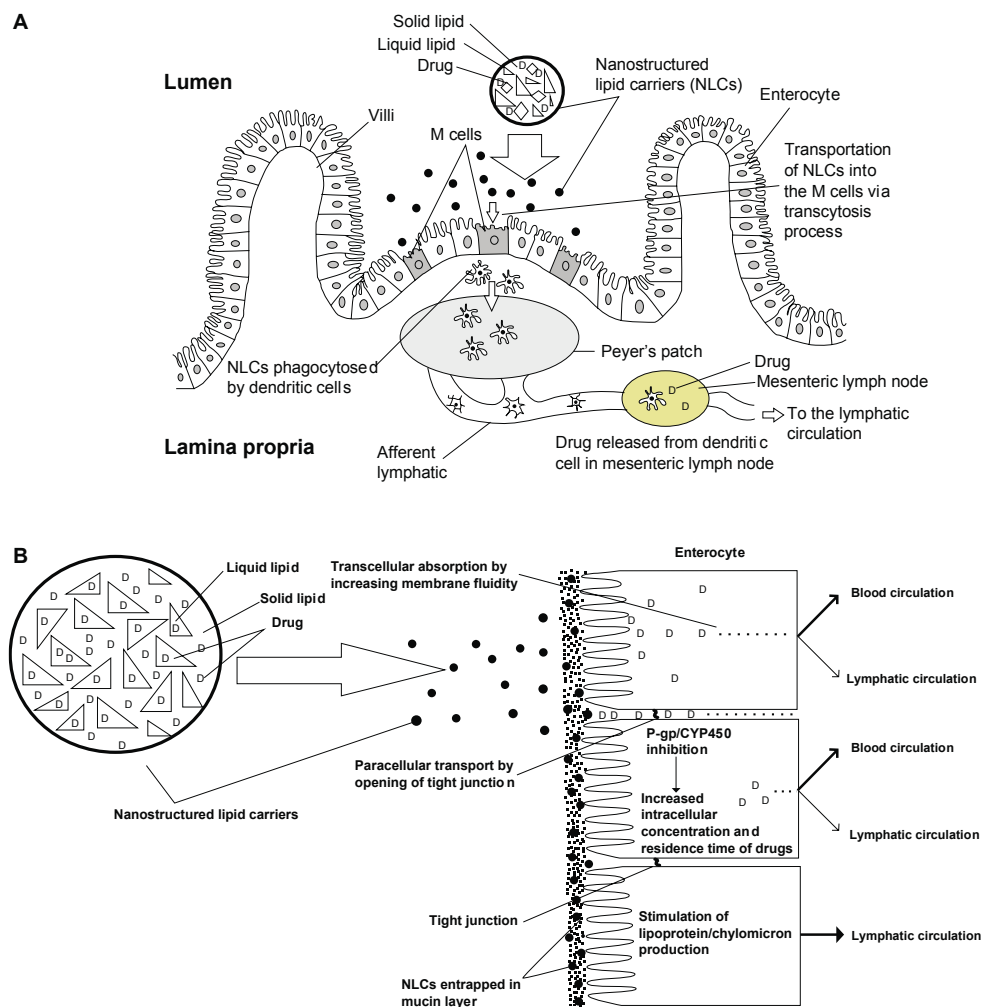


Figure 1.1 A Schematic transverse section of Peyer's patch, illustrating M cell transportation of lipid based formulation (nanostructured lipid carriers) to the lymphatic vessels. B Schematic diagram of the different mechanisms of the intestinal transport of lipid based formulation (nanostructured lipid carriers) through blood and lymphatic circulation. Adopted from Khan et al., (2013).

Abbreviations: P-gp, P-glycoprotein; CYP450, cytochrome P450 enzyme; M cell, membranous cell.

A number of lipid-based formulations, including emulsions, micellar systems, self-emulsifying drug delivery systems, self-microemulsifying drug delivery systems, self-nanoemulsifying drug delivery systems, liposomes, solid lipid nanoparticles (SLNs), and nanostructured lipid carriers (NLCs) have been investigated as drug carriers for the lymphatic system (table 1.1).

Table 1.1 Formulations that have been used for lymphatic delivery

Formulations	Drugs	References
Emulsion	Penclomedine	(Myers & Stella, 1992)
Emulsion	Ontazolast	(Hausse et al., 1998)
Microemulsion	Puerarin	(Wu et al., 2011)
Microemulsion	Raloxifene	(Thakkar et al., 2011)
Micellar systems	Cyclosporine A	(Takada et al., 1986)
SEEDS	Coenzyme Q 10	(Kommuru et al., 2001)
SMEDDS	Halofantrine	(Holm et al., 2003)
SMEDDS	Nobiletin	(Yao et al., 2008)
SMEDDS	Valsartan	(Dixit et al., 2010)
SMEDDS	Vinpocetine	(Y. Chen et al., 2008)
SMEDDS	Silymarin	(Li et al., 2010)
SMEDDS	Sirolimus	(Minghui Sun et al., 2011)
SNEDDS	Carvedilol	(Singh et al., 2011)
SNEDDS	Valsartan	(Beg et al., 2012)
SNEDDS	Halofantrine	(Holm et al., 2012)
Liposomes	IgG1	(Moghimi & Moghimi, 2008)
Liposomes	Doxorubicin	(Frenkel et al., 2006)
Liposomes	Cefotaxime	(Ling et al., 2006)
Liposomes	9-nitro-camptothecin	(Lawson et al., 2004)
Liposomes	Paclitaxel	(Latimer et al., 2009)
Liposomes	Ovalbumin	(Kojima et al., 2008)
SLNs	Etoposide	(Harivardhan et al., 2005)
SLNs	Methotrexate	(Paliwal et al., 2009)
SLNs	Idarubicin	(Zara et al., 2002a)
SLNs	Tobramycin	(Cavalli et al., 2000; Cavalli et al., 2003)

SLNs	Nimodipine	(Chalikwar et al., 2012)
NLCs	Testosterone	(Muchow et al., 2011)
NLCs	Vinpocetine	(Zhuang et al., 2010)
NLCs	Triptetine	(Zhou et al., 2012)

Abbreviations: SEEDS, Self emulsifying drug delivery system; SMEDDS, Self-microemulsifying drug delivery systems; SNEDDS, Self-nanoemulsifying drug delivery systems; SLNs, Solid lipid nanoparticles; NLCs, Nanostructured lipid carriers.

1.5 Different routes for NLCs lymphatic uptake

Lipid based nanoformulations such as SLNs and NLCs offer a prominent advantage over other nanoparticulate systems because they use physiological lipids and surfactants, which are generally recognized as safe. The commonly used lipids in the lipid based nanoformulations preparation are fatty acids, waxes, monoglycerides, diglycerides, and triglycerides; surfactants such as poloxamer and polysorbate are also widely used. Further, the possibility of avoiding a solvent using high-pressure homogenization can help to prevent the carrier biotoxicity problem in humans (Müller et al., 2000; Wissing et al., 2004). Lipid based nanoformulations involve formation of a relatively rigid core consisting of lipids that are solid at room temperature. Thus, lipid based nanoformulations can help improve stability and provide controlled release and drug targeting (Mehnert & Mäder, 2001). The minute size of these formulations enables efficient uptake of drugs into the intestine, particularly via the lymphatic route, involving particles only 20–500 nm in diameter (Yuan, Wang, et al., 2007). Absorption via the lymphatic route can be used for delivery of cytotoxic agents to overcome the limitations of nonspecificity, drug resistance, and severe toxicity (Wong et al., 2007).

There are mainly three different routes have been explored for lymphatic uptake of NLCs, including the subcutaneous, pulmonary, and duodenal routes.

1.5.1 Subcutaneous route for lymphatic delivery of NLCs

The subcutaneous route is an attractive one for lymphatic delivery of NLCs, with several advantages, including drug accumulation at the site of administration for a longer period of time, low clearance, sustained release, and increased absorption. On subcutaneous administration, NLCs are not directly transported into the bloodstream because capillaries control the permeability of water and small molecules. Instead, the lymphatic capillaries surrounding the subcutaneous injection site absorb the lipid-based nanoparticles. Absorption of NLCs into the lymphatic system depends primarily on the size of the nanoparticles. Larger NLCs accumulate at the injection site, and the drug is slowly released from the NLCs. The free drug can enter the blood circulation via pores on the walls of the capillaries. Smaller NLCs (not more than 100 nm) can easily access the lymphatic capillaries and concentrate in regional lymph nodes (Oussoren, 2001). Thus, based on these advantages, NLCs could be developed as a carrier for lymphatic drug delivery by subcutaneous administration because they have improved physicochemical properties compared with other lipid-based nanocarrier systems.

1.5.2 Pulmonary route for lymphatic delivery of NLCs

Drug administration via the pulmonary route has several advantages compared with the oral and parenteral routes. The pulmonary route avoids first-pass metabolism, reduces systemic toxicity, noninvasive, minimizes the need for continuous dosing,

allows the drugs administered to reach less accessible parts of the lung directly, and enables increased local concentrations of drug (Walker et al., 2009). The pulmonary route shows great potential for the delivery of NLCs into the lymphatic circulation. The particle size of NLCs can be reduced to less than 500 nm, which could increase drug deposition in the lung epithelium because of their diffusional mobility (Jaques & Kim, 2000). NLCs are lipid-based nanoparticles that could be used as a carrier for targeting drugs to small cell lung cancer and human immunodeficiency virus, both of which spread through the lymphatic system and can cross into the systemic circulation (Chambers et al., 2002; Pantel & Brakenhoff, 2004). Thus, NLCs have the potential to provide a drug delivery mechanism via the lymphatic system through the pulmonary route and may have increased effectiveness compared to SLNs.

1.5.3 Intestinal route for lymphatic delivery of NLCs

NLCs have the potential to be an effective method for oral drug delivery, because they can increase solubility and enhance the oral bioavailability of drugs that are either hydrophobic or poorly soluble in water (O'Driscoll & Griffin, 2008). Among the traditional lipid-based formulations, NLCs have become an important alternative to the more traditional colloidal drug carriers (Müller et al., 2002a). Zhuang et al developed drug-loaded NLCs to improve the oral bioavailability of vinpocetine (Zhuang et al., 2010). Both vinpocetine-loaded NLCs and a vinpocetine suspension were orally administered to male Wistar rats. The time taken to reach maximum plasma concentrations (t_{max}) and the peak concentration reached (C_{max}) for the vinpocetine suspension were 30 minutes and 354.29 ± 57.49 ng/mL, respectively, whereas the t_{max} and C_{max} of vinpocetine-loaded NLCs were 1.5 hours and 679.29 ± 135.57 ng/mL, respectively. The T_{max} for vinpocetine-loaded NLCs was one hour

longer than the vinpocetine suspension, indicating indirect transport of NLCs into the systemic circulation. The C_{\max} for vinpocetine-loaded NLCs was also significantly higher than the vinpocetine suspension. The area under the curve for the vinpocetine-loaded NLCs was 3.2-fold greater than that of the vinpocetine suspension. *In vivo* pharmacokinetic analysis showed a 322% increase in the relative bioavailability of vinpocetine-loaded NLCs compared to the vinpocetine suspension after oral administration. These results suggest that NLCs can improve the oral bioavailability of drug which are poorly soluble in water (Zhuang et al., 2010). One possible reason for the enhanced bioavailability of vinpocetine could be that NLCs are transported in the lymphatic system, so largely avoid first-pass metabolism, which is the main cause for the low bioavailability of vinpocetine (Zhuang et al., 2010).

In another study, Zhou et al., (2012) developed tripterine NLCs and evaluated their potential as an oral drug delivery system. A rat intestinal perfusion model was used to compare the absorption of tripterine-loaded NLCs with that of a tripterine solution. The effective permeability of tripterine NLCs in the duodenum, jejunum, ileum, and colon was 2.1, 2.7, 1.1, and 1.2 times higher, respectively, compared with the tripterine solution. The percentage absorption of tripterine-loaded NLCs in 10 cm of duodenum, jejunum, ileum, and colon was 2.2, 2.3, 1.2, and 1.3 times greater, respectively, than for the tripterine solution (Zhou et al., 2012). These results indicate that NLCs could be used as a carrier to improve the absorption of tripterine in the gastrointestinal tract.

1.6 *In vitro* models for studying lymphatic drug transport

Various *in vitro* models can serve as an alternative to *in vivo* models for studying lymphatic drug transport. In the intestinal permeability model, Caco-2 cells are used to evaluate intracellular lipoprotein-lipid assembly and to examine the effect of lipids and lipidic excipients on incorporation of drug with lipoproteins in lymphatic transport (Seeballuck et al., 2003; Seeballuck et al., 2004; Karpf et al., 2006). In one *in vitro* model, Gershkovich & Hoffman, (2005) described a correlation between the degree of ex-vivo incorporation of a drug into chylomicrons and the extent of intestinal lymphatic drug transport. According to a lipolysis model described by Dahan & Hoffman, (2008) *in vivo* drug absorption could be predicted by evaluating drug release from a lipid-based drug delivery system and estimating precipitation of the drug during lipolysis. Holm & Hoest, (2004) reported an *in silico* method that established a quantitative relationship between the molecular structure and amount of drug transferred from the intestinal to the lymphatic system.

1.6.1 *In vitro* cellular uptake study via Caco-2 cell monolayer model to evaluate the indirect lymphatic uptake of NLCs

The Caco-2 cell line is a heterogeneous human epithelial colorectal adenocarcinoma cells that derived from human colon carcinoma. These cells have the ability to differentiate and polarized functionally and morphologically as the intestinal enterocytes lining when cultured in specific conditions. These cells resemble as enterocytes in various aspects of its properties such as microvilli, tight junction, some transporters and enzymes. Due to the uniqueness of these cells and lack of proper *in vitro* lymphatic absorption methods these cells have been chosen and used as an

indirect method for the lymphatic uptake study for oral lipid based nanoformulations (Shah et al., 2014).

1.6.2 Characteristics of Caco-2 cells

1.6.2(a) Tight junction

The Caco-2 monolayers form the tight junction when cells become confluent. The integrity of monolayer can be measured by trans-epithelial electrical resistance (TEER) and paracellular markers permeability such as mannitol, inulin and lucifer yellow across the Caco-2 monolayer (Mukherjee et al., 2008). For paracellular transport the pore radius of Caco-2 tight junction is smaller ($\sim 4.5 \text{ \AA}$) than the human intestinal enterocytes tight junction pore radius ($\sim 8 - 13 \text{ \AA}$) (Fine et al., 1995; Watson et al., 2001).

1.6.2(b) Drug transporters

Several transporter and enzyme are present in Caco-2 monolayers same as found in intestine. These are H⁺/di-tripeptide transporter (PEPT1), monocarboxylic acid transporter 1 (MCT1), organic anion-transporting polypeptide 2B1 (OATP-B), organic cation/carnitine transporter (OCTN2) and apical Na⁺-dependent bile acid transporter (ASBT), all are expressed on apical membrane. Also, the efflux transporter P-glycoprotein (MDR1) and multidrug resistance-associated protein 2 (MRP2) are present on apical membrane (Figure 1.2). These efflux transporter promotes the elimination of solute from intracellular site to the basolateral area, as a result to enhance the drug absorption (Sun et al., 2008).

1.6.2(c) Metabolic enzymes

The Caco-2 monolayers express several metabolic enzymes, for example cytochrome P450 1A (CYP1A), UDP-glucuronosyltransferases (UGTs), glutathione S-transferases (GSTs) and sulfotransferases (SULTs) (figure 1.2). However, the Cytochrome P450 3A4 (CYP3A4) usually absent or weakly present in Caco-2 monolayers (Sun et al., 2008).

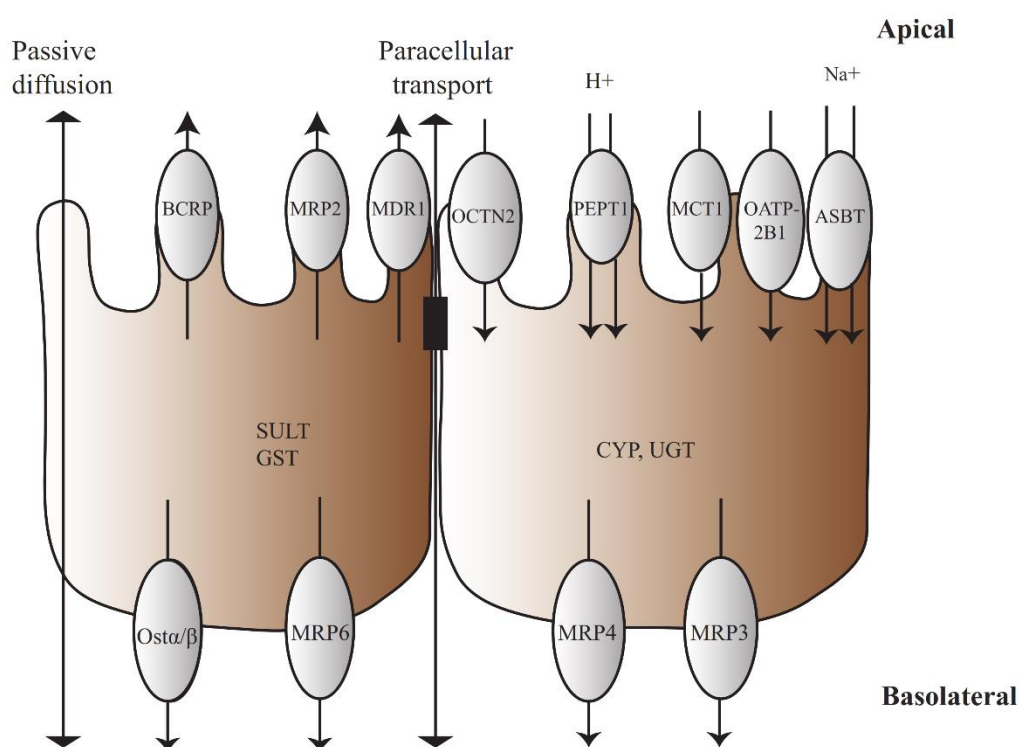


Figure 1.2 Drug transporters and metabolic enzymes present in Caco-2 cell monolayer

Abbreviations: PEPT1, H⁺/di-tripeptide transporter; OATP-B, organic anion-transporting polypeptide 2B1; MCT1, monocarboxylic acid transporter 1; ASBT, Na⁺-dependent bile acid transporter; OCTN2, organic cation/carnitine transporter; MDR1, or P-glycoprotein, P-gp, multidrug resistance protein 1; MRP2, multidrug resistance-associated protein 2; MRP3, multidrug resistance-associated protein 3; MRP4, multidrug resistance-associated protein 4; MRP6, multidrug resistance-associated protein 5; BCRP, breast cancer resistance protein; OSTα/β, organic solute transporters; CYP, cytochrome P450; SULTs, sulfotransferases; UGTs, UDP-glucuronosyltransferases; GSTs, glutathione S-transferases.